



PRODUCTION ENGINEERING ARCHIVES

 ISSN 2353-5156 (print)
 ISSN 2353-7779 (online)

 Exist since 4th quarter 2013
 Available online at www.pea-journal.eu

Formation of coatings with technologies using concentrated energy stream

Norbert Radek^{1,*}, Artur Kalinowski¹, Jacek Pietraszek², Lukasz J. Orman¹,
 Marcin Szczepaniak³, Adam Januszko⁴, Janusz Kamiński⁵, Jozef Bronček⁶, Olga Paraska⁷

¹ Kielce University of Technology, al. 1000-lecia P.P. 7, 25-314 Kielce, Poland; akalinowski@tu.kielce.pl (AK); orman@tu.kielce.pl (ŁO)

² Cracow University of Technology, Al. Jana Pawła II 37, 31-864 Kraków, Poland; jacek.pietraszek@mech.pk.edu.pl

³ Military Institute of Engineer Technology, 50-961 Wrocław, Poland; szczepaniak@witi.wroc.pl

⁴ Military University of Land Forces, ul. Piotra Czajkowskiego 109, 51-147 Wrocław, Poland; adam.januszko@awl.edu.pl

⁵ Warsaw University of Technology, Plac Politechniki 1, 00-661 Warszawa, Poland; janusz.kaminski@pw.edu.pl

⁶ University of Zilina, Univerzitna 1, 01026 Zilina, Slovakia; jozef.broncek@fstroj.uniza.sk

⁷ Khmelnytskyi National University, st. Instytutaska 11, 29016, Khmelnytskyi, Ukraine; olgaparaska@gmail.com

*Correspondence: norrad@tu.kielce.pl

Article history

Received 09.12.2021

Accepted 20.01.2022

Available online 23.05.2022

Keywords

Electro-spark deposition

Laser beam processing

Coating

Heterogeneous surface

DOI: 10.30657/pea.2022.28.13

Abstract

A number of modern surface processing methods use an energy flux. The examples include electro-spark deposition (ESD) and laser beam processing (LBP). The work concerns the study of Cu-Mo coatings deposited on C45 carbon steel, which were then eroded with a laser beam. The analysis included the analysis of the microstructure, measurements of macrogeometry and microhardness, corrosion resistance tests of selected areas after laser treatment. The coatings were applied with ELFA-541 and subjected to Nd:YAG laser treatment with variable laser parameters. The problem presented in the work can be used to extend the knowledge of the areas of application of ESD coatings, especially in sliding friction pairs.

JEL: L69, M11

1. Introduction

During tribological investigations it was found that employing heterogeneous surfaces models into boundary interaction of solid surfaces could make significant improvement (Ryk et al., 2006). Surfaces described as heterogeneous consist of areas, which are different one from another in geometrical, physicomechanical or physicochemical properties. The heterogeneity of surfaces is frequently due to the application of more than one technology, and can be constituted by (Wan et al., 2008):

- shaped surface features such as grooves, pits or channels resulting from milling, eroding, etching, laser-beam forming, etc.,
- areas with different physicochemical and physicomechanical properties, e.g. areas with varying hardness and mechanical strength accomplished by local surfacing or selective surface hardening (e.g. electron-beam machining, laser-beam forming or thermochemical treatment),

- areas with diversified surface microgeometry, e.g. areas eroded at the points of focus (laser treatment or electro-spark deposition), or areas with formed surface microgeometry, for instance, in terms of desired microroughness directivity or load capacity (laser beam processing and electro-spark deposition technologies).

Heterogeneous surfaces can be obtained by different methods. The laser treatment of electro-spark deposited coatings being one of them (Antoszewski et al., 2005; Radek, 2010).

The process of material growth resulting from electro-erosion is known as electro-spark alloying (ESA) or electro-spark deposition (ESD). The erosion of the anode and the spark discharges between the electrodes result in the formation of a surface layer with properties different from those of the base material (Padgurskas et al., 2017; Salmaliyan et al., 2017; Aghajani et al., 2020).

However, it is possible to improve the quality of the coating using appropriate laser beam processing (Gadek-Moszczak et al., 2014; Radek et al., 2015, 2018). The coating structure is modified by the laser beam, which also significantly affects its mechanical and functional properties.

It should be expected that the advantages of laser beam processing (LBP) of ESD coatings would include the following:

- improvement of the smoothness of the coating surface,
- reduction of coating porosity,
- improvement of the adhesion of the coating to the substrate material,
- increased wear resistance and galling,
- reduction of adverse tensile stresses which will increase fatigue strength,
- increased corrosion resistance.

The aim of the study was to determine selected surface properties of Cu-Mo coatings after laser treatment.

It is assumed that the use of laser-modified electro-spark deposited coatings will increase the applications of using relatively inexpensive materials in areas requiring special alloys. Designers of devices exposed to corrosion may be interested in the results, including in the field of biotechnology (Skrzypczak et al., 1994; Skrzypczak-Pietraszek and Hensel, 2000), implants (Dudek and Kolan, 2010; Dudek and Włodarczyk, 2010), but also ventilation (Kulis and Müller, 2020), power boilers (Guidoni et al., 2005), heat exchangers (Orman, 2009; Styrylska and Pietraszek, 1992) and power hydraulics (Filo et al., 2018). The article should also inspire alternative coating methods (Klimecka-Tatar et al., 2010; Maruszczuk et al., 2017) and researchers of wear issues in the railway (Mysiek, 2020) and machine industry (Ulewicz et al., 2014; Pacana et al., 2019; Rączka et al., 2020; Markovic et al., 2021), especially military (Dziopa and Koruba, 2015; Krzysztofik et al., 2017, Szczodrowska and Mazurczuk, 2021), which are inextricably linked with quality management (Ostasz et al., 2020; Fabiś-Domagala et al., 2021). Finally, it will undoubtedly have an impact on analogous experimental studies (Przestacki et al., 2017; Galin et al., 2021), thermal resistance (Zajdel, 2021) and related analytical methods (Dwornicka et al., 2017).

2. Experimental

The testing process consisted of two stages: first, Cu-Mo coatings were electro-spark deposited on standard steel samples (C45 carbon steel); then, they were modified with a laser beam. The electro-spark deposition of Cu-Mo wires with a diameter of 1 mm was performed by means of an ELFA-541, a modernized device made by a Bulgarian manufacturer. The subsequent laser treatment was performed with the aid of a BLS 720 laser system employing the Nd:YAG type laser operating in the pulse mode.

The parameters of the electro-spark deposition, established during the experiment, include: current intensity $I = 16$ A (for Cu $I = 8$ A); table shift rate $v = 0.5$ mm/s; rotational speed of the head with electrode $n = 4200$ rev/min; number of coating passes $L = 2$ (for Cu $L = 1$); capacity of the condenser system $C = 0.47$ μ F; pulse duration $T_i = 8$ μ s; interpulse period $T_p = 32$ μ s; frequency $f = 25$ kHz.

The produced heterogeneous coatings were eroded by laser beam after the electro-spark deposition. The laser surface treatment was performed by an Nd:YAG laser (impulse

mode), model BLS 720, and operating in the pulse mode under the following conditions:

- laser spot diameter, $d = 0.462$ - 0.739 mm,
- laser power, $P = 10$ - 150 W,
- beam shift rate, $v = 1200$ mm/min,
- nozzle-sample distance, $h = 1$ mm,
- pulse duration, $t_i = 0.8$ ms, 1.2 ms, 1.48 ms, 1.8 ms, 5.5 ms, 8 ms,
- frequency, $f = 8$ Hz.

The main objectives of the investigations were:

- observing the surface state by means of a stereoscopic microscope,
- microstructure analysis by means of a scanning electron microscope,
- analyzing the surface macrogeometry,
- measuring the microhardness with the Vickers method,
- corrosion resistance tests.

3. Results and discussion

A microstructure analysis was conducted for ESD coating systems using the JEOL JSM-7100F scanning electron microscope with field emission. Figure 1 shows the image of the top surface of Cu-Mo coating on C45 carbon steel surface. The splash appearance, micro-cracks and spattering particles can be seen. Molten droplets formed on the electrode tip during the heating process. The droplets are accelerated by high current plasma and impinge on the substrate surface resulting in the splash in different directions.

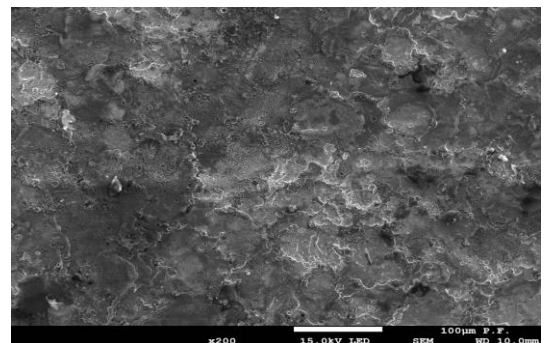


Fig. 1. Image of the top surface of Cu-Mo coating on the C45 carbon steel surface

Figures 2 show the microstructure of electro-spark deposited two-layer Cu-Mo coatings. The layer thickness is approximately 8 - 10 μ m, and the range of the heat affected zone (HAZ) inside the (underlying) substrate material is about 10 - 15 μ m. In the photograph, the boundary line between the two-layer coating and the substrate is clear. The melting and solidifying processes during laser treatment resulted in the migration of elements across the coating-substrate interface. Laser radiation caused intensive convective flow of the liquid material in the pool and, in consequence, the homogenization of the chemical composition (Fig. 3). In the heat affected zone (HAZ), which was 20 - 50 μ m thick, there was an increase in the content of carbon.

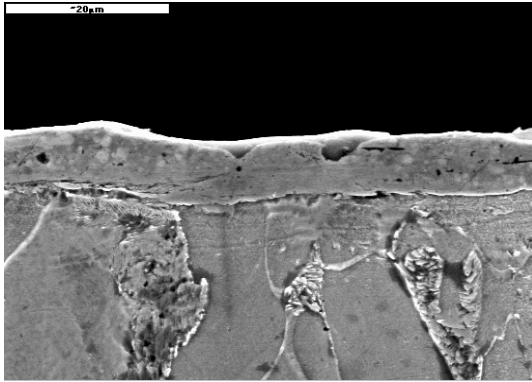


Fig. 2. Microstructure in the Cu-Mo coating

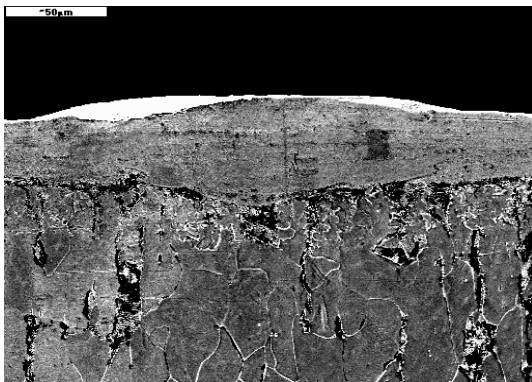


Fig. 3. Microstructure in the Cu-Mo coating after laser treatment

The Cu-Mo coatings structure after electro-spark deposition on steel coupons and eroded by laser beam were investigated. The observation was done by OLYMPUS SZ-STU2 stereoscopic microscope.

As can be seen from Figures 4 and 5, the effect of the laser erosion action is in the form of craters. The first one is showing lower laser power ($P = 20$ W) interaction effect on the treated surface (Fig. 4). The second one is illustrating phenomenon (Fig. 5), where the laser power was increased 5 times ($P = 100$ W). The cavity depth depends mainly on the laser power density and the pulse duration. Coatings with such geometry have various tribological applications. By rubbing the surface selectively, it is possible to produce cavities inside which hydrodynamic forces can be generated during fluid film lubrication. Moreover, the hard areas around the cavities are capable of bearing normal loads.

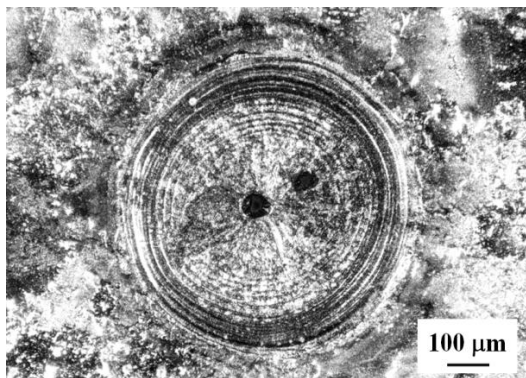


Fig. 4. Stereoscopic photograph of a Cu-Mo coating laser-eroded at 100 W

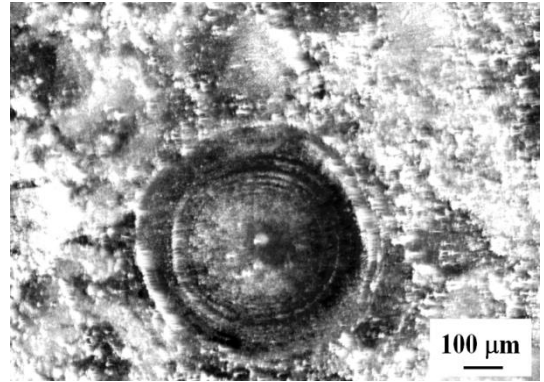


Fig. 5. Stereoscopic photograph of a Cu-Mo coating laser-eroded at 20 W

The investigations of the effects of the laser erosion involved measuring the diameters and depths of the cavities obtained at different laser powers. The results of the measurement performed with a PG-2/200 form surfer are presented in the form of graphs in Figure 6. It was noticed that higher laser beam power gives greater diameter and depth of the cavities. An exception is the cavity depth produced at 150 W. The value is smaller than that obtained at 100 W. This might have been due to a considerable pulse duration ($t_i = 8$ ms), the laser power being 150 W. However, if $P = 100$ W, the pulse duration t_i was 5.5 ms. In the case of lasers operating in the pulse mode, the power is averaged in time; thus, if the pulse durations are long, the laser beam is less effective.

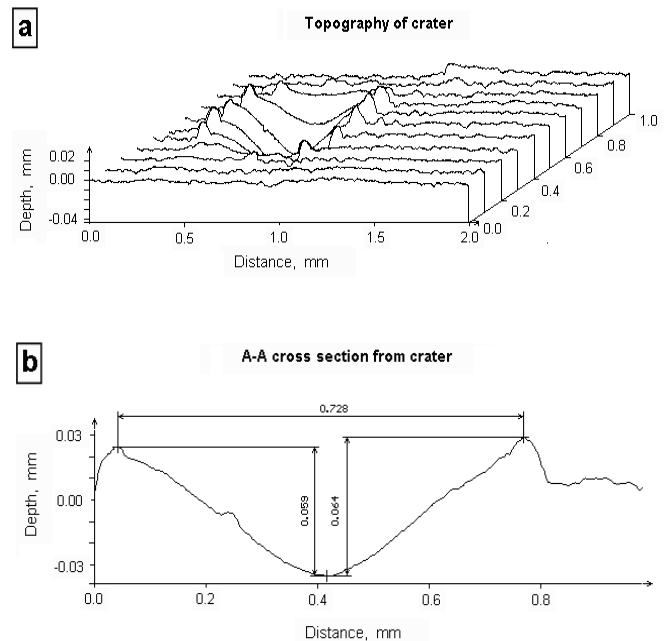


Fig. 6. Macroeometry and cross section of a crater eroded by laser: a) 3D crater topography; b) A-A cross section on Figure 4

A 3D macrogeometry of the developed heterogeneous surface eroded by the laser craters for the used specimens with build in 2-D crater cross section A-A (Fig. 4) is shown in Figures 6a and 6b. As can be concluded from these graphs, crater edges are sharp and are protruding 0.03 mm above an average height, just treated by ESD surface, what is within a range of tolerances for designed clearance fit. The average size of the

crater shown on Figure 4 produced by laser power 100 W is about 0.7 mm in diameter and the total depth about 0.06 mm. The crater is going below so-called “ground zero level” by down to 0.030 mm. For instance, crater displayed in Figure 5, produced by laser power 20 W, is about 0.05 mm in diameter and has a depth of 0.015 mm. Produced crater profile (picks and valleys) and also order of craters location, depending on the required or desired surface performance, could be controlled and adjusted to acceptable level. can be seen from Figure 7, relationship of the eroded cavity diameters and related cavity depth mainly depends on the laser power and pulse duration.

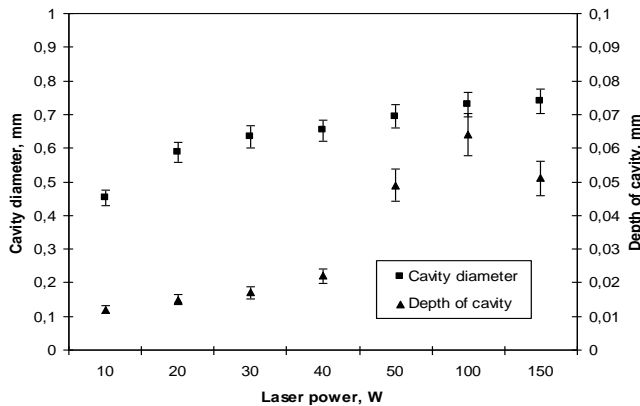


Fig. 7. Relation of laser craters depth and laser power

At the next stage, the Vickers microhardness test was conducted using a load of 0.98 N. The measurements was carried out on Cu-Mo coatings laser-eroded at 20 W. The distribution of microhardness is shown in Figure 8.

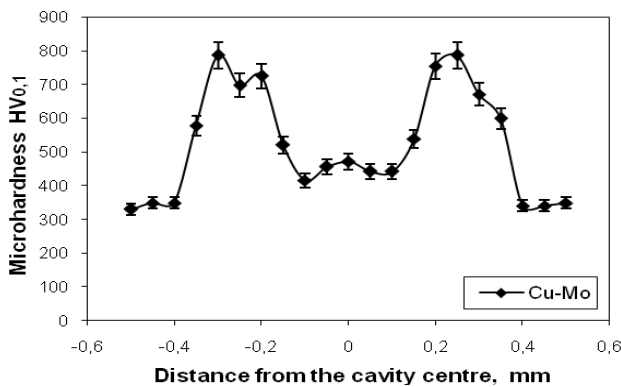


Fig. 8. Distribution of microhardness on the surface of a laser-treated Cu-Mo coating

It was established that there was an increase in microhardness at the points of laser machining, the increase being strictly related to the changes in the coating structure, and therefore, to the method of laser treatment. The surface hardening at the points of laser interaction and in the heat-affected zone (HAZ) follows the phase changes occurring in the material first heated and then immediately cooled. The average microhardness of the C45 steel substrate was 300 HV. That of the ESD coatings amounted to about 430 HV. The laser treatment of the ESD coatings caused an increase in microhardness

to approximately 850-880 HV. In the heat-affected zone, the microhardness fluctuated around 580-630 HV. The laser beam surface forming resulted in changes in the microhardness of electro-spark deposited Cu-Mo coatings.

In the last stage of the research, corrosion resistance tests were carried out. The corrosion resistance of Cu-Mo coating before and after laser treatment was evaluated by electrochemical test. A variable potential method was applied, which is accepted as effective method of electrochemical testing. The cathode polarization curve and the anode polarization curve were determined by polarizing the samples with a potential shift rate of 0.2 mV/s, and the range of ± 200 mV of the corrosive potential, and 0.4 mV/s in at higher potential. Samples with a marked area of 10 mm in diameter were polarized up to a potential of 500 mV. The polarization curves were drawn for samples immersed for 24 hours into a 3.5% NaCl solution so that the corrosive potential could be established. The tests were performed at a room temperature of 21°C ($\pm 1^\circ\text{C}$).

Curves of the Cu-Mo coating polarization, before and after the laser treatment, are shown in Figure 9. The characteristic electrochemical values of the materials under test are presented in Table 1.

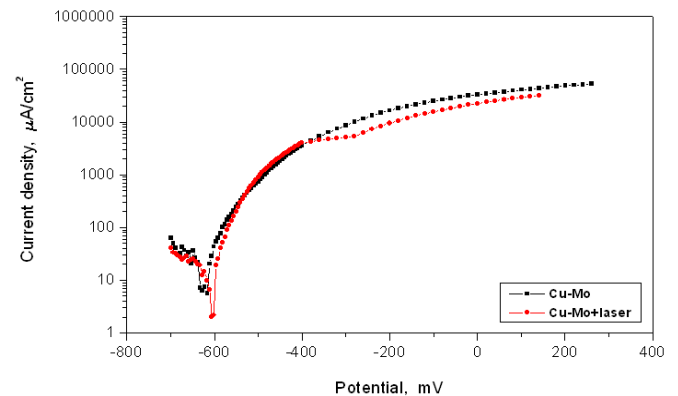


Fig. 9. Curves of the Cu-Mo coating polarization before and after laser treatment

Table 1 indicates that Cu-Mo coating has high corrosion resistance, relative to the substrate steel. The corrosion current density of the Cu-Mo coating was 42.9 $\mu\text{A}/\text{cm}^2$. In comparison, the substrate material C45 steel was 112 $\mu\text{A}/\text{cm}^2$, which is a significant improvement. However, there is relatively only a small improvement in the corrosion resistance of the electro-spark deposited coatings after laser treatment. The improvement by laser treatment can be explained by the healing of microcracks, and therefore, better sealing properties.

Table 1. Current density and corrosion potential of the tested materials

Material	Corrosion current density I_k [$\mu\text{A}/\text{cm}^2$]	Corrosion potential E_{KOR} [mV]
C45 carbon steel	112 \pm 17.8%	-458
Cu-Mo	42.9 \pm 11.8%	-620
Cu-Mo+Laser	30.7 \pm 2.6%	-629

4. Conclusions

Based on the obtained test results and their interpretation, the following conclusions can be drawn:

1. Heterogeneous surface is made by ESD coating and post finished selectively by laser erosion.
2. Developed surface has fusion and substrate structural zones. The fusion zone presents of great interest and comprises of three layers. The outmost layer approaches quenched like structure and exhibit homogeneity and high micro hardness readings.
3. Laser irradiation of coatings resulted in the healing of micro-cracks and pores.
4. Laser treatment caused a 51% increase in the micro-hardness of the electro-spark deposited Cu-Mo coatings.
5. The laser processed ESD Cu-Mo coatings show improved resistance to corrosion (by 28%).
6. The surface heterogeneity (i.e. the cavities) are desirable in sliding friction pairs. They may be used as reservoirs of lubricants as well as sources of hydrodynamic forces increasing the capacity of a sliding pair.
7. Further research should involve tribological tests of electro-spark coatings before and after laser treatment.

Reference

- Aghajani, H., Hadavand, E., Peighambari, N.S., Khameneh-asl, S., 2020. Electro spark deposition of WC-TiC-Co-Ni cermet coatings on St52 steel. *Surfaces and Interfaces*, 18.
- Antoszewski, B., Radek, N., Tarelnik, W., Wajs, E., 2005. Electro discharge and laser texturing of sliding face of mechanical seals. IX International Conference HERVICON, Sumy, Ukraine, 15-123.
- Dudek, A., Kolan, C., 2010. Assessments of Shrinkage Degree in Bioceramic Sinters HA+ZrO(2). *Mechatronic Systems and Materials: Materials Production Technologies*, 165, 25-30.
- Dudek, A., Włodarczyk, R., 2010. Structure and Properties of Bioceramics Layers used for Implant Coatings. *Solid State Phenomena*, 165, 31-36.
- Dwornicka, R., Radek, N., Krawczyk, M., Osocha, P., Pobedza, J., 2017. The Laser Textured Surfaces of the Silicon Carbide Analyzed with the Bootstrapped Tribology Model. *METAL 2017*, 26th International Conference on Metallurgy and Materials, 1252-1257.
- Dziopa, Z., Koruba, Z., 2015. The impact of launcher turret vibrations control on the rocket launch. *Bulletin of the Polish Academy of Sciences-Technical Sciences*, 63(3), 717-728.
- Fabiś-Domagala, J., Domagala, M., Momeni, H., 2021. A matrix FMEA analysis of variable delivery vane pumps. *Energies*, 14(6), art. 1741.
- Filo, G., Lisowski, E., Domagala, M., Fabiś-Domagala, J., Momeni, H., 2018. Modelling of Pressure Pulse Generator with the Use of a Flow Control Valve and a Fuzzy Logic Controller. *AIP Conf. Proc.*, 2029, art. 020015.
- Gadek-Moszczak, A., Radek, N., Wroński, S., Tarasiuk, J., 2014. Application the 3D Image Analysis Techniques for Assessment the Quality of Material Surface Layer before and after Laser Treatment. *Advanced Materials Research.*, 874, 133-138.
- Galini, R., Khina, B., Shaburova, N., Wassilkowska, A., 2021. The formation of zinc coatings in nanocrystallised zinc powders. *Technical Transactions*, 118, art. e2021009, DOI: 10.37705/TechTrans/e2021009
- Guidoni, G., Dudek, A., Patsias, S., Anglada, M., 2005. Fracture behaviour of thermal barrier coatings after high temperature exposure in air. *Materials Science and Engineering A*, 397(1-2), 209-214.
- Klimecka-Tatar, D., Pawłowska, G., Szymura, S., 2010. Encapsulation as an effective prevention method of powder oxidation in bonded magnet technology. *Ochrona Przed Korozją*, 53(11), 585-588.
- Krzysztofik, I., Takosoglu, J., Koruba, Z., 2017. Selected methods of control of the scanning and tracking gyroscope system mounted on a combat vehicle. *Annual Reviews in Control*, 44, 173-182.
- Kulis, C., Müller, J., 2020. Indoor air quality improvement in natural ventilation using a fuzzy logic controller. *Technical Transactions*, 117, art. e2020045, DOI: 10.37705/TechTrans/e2020045
- Markovic, S., Arsic, D., Nikolic, R.R., Lazic, V., Hadzima, B., Milovanovic, V.P., Dwornicka, R., Ulewicz, R., 2021. Exploitation Characteristics of Teeth Flanks of Gears Regenerated by Three Hard-Facing Procedures. *Materials*, 14(15), art. 4203.
- Maruszczak, A., Dudek, A., Szala, M., 2017. Research into Morphology and Properties of TiO₂ - NiAl Atmospheric Plasma Sprayed Coating. *Advances in Science and Technology-Research Journal*, 11(3), 204-210.
- Myslek, A., 2020. Crack propagation analysis in selected railway bogie components. *Technical Transactions*, 117, art. e2020017, DOI: 10.37705/TechTrans/e2020017
- Orman, L. J., 2009. Possibilities of Heat Transfer Enhancement in Automotive Heat Exchangers, *Transport Means 2009*: 116-119.
- Ostasz, G., Czerwinska, K., Pacana, A., 2020. Quality Management of Aluminum Pistons with the Use of Quality Control Points, *Management Systems in Production Engineering*, 28(1), 29-33.
- Pacana, A., Czerwinska, K., Dwornicka, R., 2019. Analysis of Non-Compliance for the Cast of the Industrial Robot Basis, 28th International Conference on Metallurgy and Materials, 644-650.
- Padgurskas, J., Kreivaitis, R., Rukuiža, R., Mihailov, V., Agafii, V., Kriūkienė, R., Baltušnikas, A., 2017. Tribological properties of coatings obtained by electro-spark alloying C45 steel surfaces, *Surface and Coatings Technology*, 311, 90-97.
- Przestacki, D., Kuklinski, M., Bartkowska, A., 2017. Influence of laser heat treatment on microstructure and properties of surface layer of Waspaloy aimed for laser-assisted machining. *International Journal of Advanced Manufacturing Technology*, 93(9-12), 3111-3123.
- Radek, N., 2010. Production of proper texture on the flat sliding pair surfaces by means of electro-erosion or laser treatment, *Mechanik*, 83(11), 822-825.
- Radek, N., Konstany, J., Scendo, M., 2015. The electrospark deposited WC-Cu coatings modified by laser treatment. *Archives of Metallurgy and Materials*, 60, 2579-2584.
- Radek, N., Szczotok, A., Gadek-Moszczak, A., Dwornicka, R., Bronček, J., Pietraszek, J., 2018. The impact of laser processing parameters on the properties of electro-spark deposited coatings. *Archives of Metallurgy and Materials*, 63, 809-816.
- Rączka, M., Pysz, S., Piotrowski, K., 2020. Guidelines for the manufacture of heavy ductile iron castings. *Technical Transactions*, 117, art. e2020044, DOI: 10.37705/TechTrans/e2020044
- Ryk, G., Etsion, I., 2006. Testing piston rings with partial laser surface texturing for friction reduction. *Wear*, 261, 792-796.
- Salmaliyan, M., Malek Ghaeni, F., Ebrahimnia, M., 2017. Effect of electro spark deposition process parameters on WC-Co coating on H13 steel. *Surface and Coatings Technology*, 321, 81-89.
- Skrzypczak, L., Skrzypczak-Pietraszek, E., Lamerzarawska, E., Hojden, B., 1994. Micropropagation of *Oenothera-Biennis* L and an Assay of Fatty-Acids. *Acta Societatis Botanicorum Poloniae*, 63(2), 173-177.
- Skrzypczak-Pietraszek, E., Hensel, A., 2000. Polysaccharides from *Melittis melissophyllum* L. herb and callus. *Pharmazie*, 55(10), 768-771.
- Styrylska, T., Pietraszek, J., 1992. Numerical Modeling of Non Steady State Temperature Fields with Supplementary Data. *Zeitschrift für Angewandte Mathematik und Mechanik*, 72(6), T537-T539.
- Szczodrowska, B., Mazurczuk, R., 2021. A review of modern materials used in military camouflage within the radar frequency range. *Technical Transactions*, 118, art. e2021003, DOI: 10.37705/TechTrans/e2021003
- Ulewicz, R., Szataniak, P., Novy, F., 2014. Fatigue Properties of Wear Resistant Martensitic Steel. *METAL 2014*: 23rd International Conference on Metallurgy and Materials, 784-789.
- Wan, Y., Xiong, D. S., 2008. The effect of laser surface texturing on frictional performance of face seal. *Journal of Materials Processing Technology*, 197, 96-100.
- Zajdel, P., 2021. A suitability assessment using an instrumented impact test of the use of selected structural steel grades on the basis of their changes in response to exposure to fire. *Technical Transactions*, 118, art. e2021007, DOI: 10.37705/TechTrans/e2021007

使用集中能量流技术形成涂层

關鍵詞

电火花沉积
激光束加工
涂层
异质表面

摘要

许多现代表面处理方法使用能量通量。示例包括电火花沉积 (ESD) 和激光束处理 (LBP)。这项工作涉及沉积在 C45 碳钢上的 Cu-Mo 涂层的研究，然后用激光束腐蚀这些涂层。分析包括显微组织分析、宏观几何和显微硬度测量、激光处理后选定区域的耐腐蚀性测试。涂层涂有 ELFA-541，并经过可变激光参数的 Nd:YAG 激光处理。工作中提出的问题可用于扩展 ESD 涂层应用领域的知识，特别是在滑动摩擦副中。
